Ab initio structural energetics of β-Si$_3$N$_4$ surfaces

Juan C. Idrobo, Hakim Iddir, and Serdar Öğüt

Department of Physics, University of Illinois at Chicago, Chicago Illinois 60607, USA

Alexander Ziegler and Nigel D. Browning

Department of Chemical Engineering and Materials Science, University of California, Davis, California 95616, USA
and Lawrence Berkeley National Laboratory, Berkeley, California 94720, USA

R. O. Ritchie

Department of Materials Science and Engineering, University of California, Berkeley, California 94720, USA
and Materials Sciences Division, Lawrence Berkeley National Laboratory, Berkeley, California 94720, USA

(Received 28 October 2005; published 2 December 2005)

Motivated by recent electron microscopy studies on the Si$_3$N$_4$/rare-earth oxide interfaces, the atomic and electronic structures of bare β-Si$_3$N$_4$ surfaces are investigated from first principles. The equilibrium shape of a Si$_3$N$_4$ crystal is found to have a hexagonal cross section and a faceted domelike base in agreement with experimental observations. The large atomic relaxations on the prismatic planes are driven by the tendency of Si to saturate its dangling bonds, which gives rise to resonant-bond configurations or planar sp^2-type bonding. We predict three bare surfaces with lower energies than the open-ring ($10\bar{1}0$) surface observed at the interface, which indicate that nonstoichiometry and the presence of the rare-earth oxide play crucial roles in determining the termination of the Si$_3$N$_4$ matrix grains.

The desirable mechanical and physical properties of silicon nitride ceramics[1] in many high temperature applications are hindered by their intrinsic brittleness, which limits their widespread use and reliability as structural components. It has been empirically known for some time that this problem can be overcome by microstructural and compositional designs with sintering additives, in particular rare-earth oxides.[2] The resulting ceramic microstructure consists of elongated Si$_3$N$_4$ matrix grains embedded in an intergranular, typically amorphous, rare-earth oxide phase. However, precise information about the structure and chemistry of the interface has been lacking for many years. Recently, there have been three experimental studies using scanning transmission electron microscopy (STEM), which revealed important information about the atomic structures and bonding characteristics at the β-Si$_3$N$_4$/rare-earth oxide interfaces.[3] This exciting development provides a timely motivation for systematic theoretical studies of the interface, which should complement and aid in the interpretation of these experiments.

Existing theoretical calculations in this field,[4] which have typically employed tight-binding, pair potential, and molecular orbital methods (a few of which are from first principles), have mainly focused on the bonding sites of additive atoms at the interface and the resulting electronic structure. While these studies have provided important information on the Si$_3$N$_4$/rare-earth oxide interface, our approach is to start with detailed first-principles calculations on *bare* Si$_3$N$_4$ surfaces, which have not yet been performed. We believe that such an approach is a natural step in a *systematic* understanding of the interface at the microscopic level. In this paper, we present results from first-principles calculations on low-index β-Si$_3$N$_4$ surfaces focusing in particular on (i) the equilibrium shape of the crystal, and (ii) the atomic structure and stoichiometry at the prismatic plane ($10\bar{1}0$) surface, which is the relevant surface studied in recent STEM experiments [Fig. 1(a)].

Our calculations were performed within density functional theory using the projector augmented wave method.[5] For exchange correlation, we used the Perdew-Wang parametrization of the generalized gradient approximation (GGA), and repeated some of the calculations using the Ceperley-Alder functional within the local-density approximation (LDA) for comparison. An energy cutoff of 270 eV was used in all calculations. For structural optimization of the bulk, a
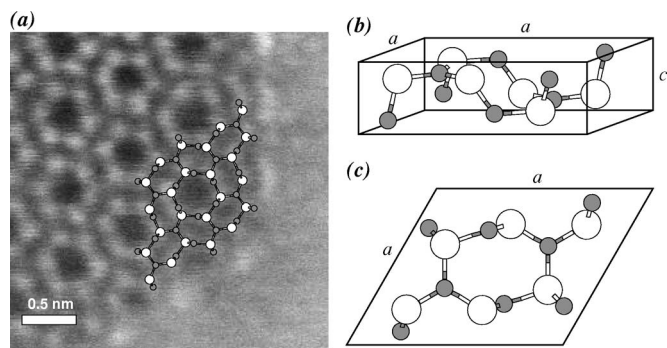

FIG. 1. (a) Z-contrast image of a Si$_3$N$_4$ grain with a hexagonal edge showing the interface with Lu$_2$O$_3$. The grain is oriented with the [0001] projection (note the superimposed atomic structure), so that the ($10\bar{1}0$) prismatic boundary planes are set at an "edge-on" condition. Lu atoms are the bright spots attached in pairs at the termination of the hexagonal open rings. (b) A perspective view of the β-Si$_3$N$_4$ unit cell. Si and N atoms are shown in white and gray circles, respectively. (c) [0001] projected view of the unit cell.

TABLE I. Supercell shape, parameters, and surface energies for the five lowest-index β-Si$_3$N$_4$ surfaces. In the second column, the numbers in parentheses are the surface unit cell dimensions; M (monoclinic) and BCM (base-centered monoclinic) refer to the lattice type of the supercell, and β is the monoclinic angle. The energies for (11$\bar{2}$0), (11$\bar{2}$1), and (10$\bar{1}$0) refer to the lowest-energy stoichiometric terminations, while the energy for (10$\bar{1}$0) is that of the open-ring surface.

Surface	Supercell	E_{surf} (J/m^2)
(10$\bar{1}$0)	(a,c), M, $\beta=60°$	2.57
(11$\bar{2}$0)	$(a\sqrt{3},c)$, M, $\beta=30°$	1.95
(0001)	(a,a), Hexagonal	2.74
(10$\bar{1}$1)	$(\sqrt{3a^2+4c^2},a)$, BCM, $\beta=66.2°$	2.77
(11$\bar{2}$1)	$(\sqrt{a^2+4c^2},a\sqrt{3})$, BCM, $\beta=52.6°$	2.81

Γ-centered $3\times3\times8$ **k**-point grid was employed. Doubling the **k**-point grid and increasing the cutoff to 400 eV had no appreciable effect on the calculated structural parameters. The hexagonal unit cell of β-Si$_3$N$_4$ contains 14 atoms with six structural parameters (a,c, and four internal parameters). Half the atoms are in the plane $z=c/4$, and the other half are in the $z=3c/4$ plane, as shown in Fig. 1(b). Si atoms are fourfold coordinated with N atoms in a slightly distorted tetrahedral configuration, and N atoms are threefold coordinated with Si atoms. The six structural parameters $(a,c,x_{Si},y_{Si},x_N,y_N)$ optimized with GGA (7.667 Å, 2.928 Å, 0.1752, 0.7692, 0.3299, 0.031) and LDA (7.585 Å, 2.895 Å, 0.1738, 0.7675, 0.3301, 0.0295) are in good agreement with previous calculations[6] and experimental values[7] of (7.608 Å, 2.911 Å, 0.1733, 0.7694, 0.3323, 0.0314). The surface calculations were performed with the relaxed structural parameters using a slab geometry. Depending on the surface, we used hexagonal and simple or base-centered monoclinic supercells (Table I). For each surface, we considered up to four different stoichiometric terminations to find the lowest-energy atomic configuration. We performed several tests to assess the convergence of the surface energy with respect to number of layers (up to 7) and the size of the vacuum region (up to 10 Å). Although the convergence was observed to be rapid [with the exception of the (11$\bar{2}$0) surface], we used five-layer slabs [10-layer for (11$\bar{2}$0)] with 8–10 Å vacuum.

Experimentally, it is observed that the Si$_3$N$_4$ microstructure consists of elongated structures with hexagonal cross sections. The preferential growth along the c axis is rather rapid, while the growth of the (10$\bar{1}$0) and (11$\bar{2}$0) prismatic planes is reaction limited and very sensitive to the type of additives.[8] In order to understand the growth process of bare Si$_3$N$_4$ grains, we calculated the surface energies of five low-index Si$_3$N$_4$ surfaces (Table I). The equilibrium shape of β-Si$_3$N$_4$ calculated from these energies by the Wulff construction[9] is shown in Fig. 2. The exposed faces consist of the {11$\bar{2}$0}, {10$\bar{1}$1}, {11$\bar{2}$1}, and {0001} families of planes making up $\sim$64%, 20%, 12%, and 4% of the total surface area, respectively. The calculated aspect ratio for bare sur-
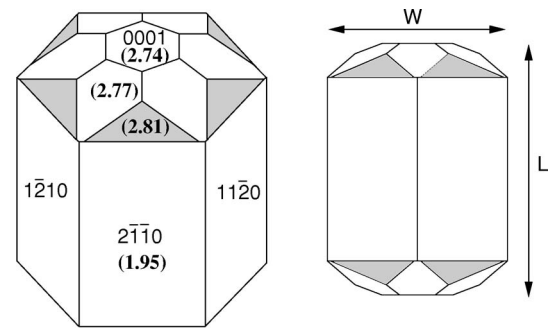

FIG. 2. Two views of the equilibrium shape of a β-Si$_3$N$_4$ crystal calculated using the Wulff construction. Four families of surfaces are exposed: {11$\bar{2}$0}, {0001}, {11$\bar{2}$1} (the shaded family of surfaces), and {10$\bar{1}$1} [the unshaded family of surfaces surrounding the (0001) surface]. The bold numbers in parentheses are the calculated surface energies in J/m^2. The calculated L/W aspect ratio is 1.4.

faces between the crystal length and its width is 1.4, which is in agreement with the measured aspect ratios near 2 for Si$_3$N$_4$ samples sintered without or only the minimum amount of the additive. We expect that in the presence of the rare-earth oxide additive, the energies of (11$\bar{2}$0) or (10$\bar{1}$0) will be lower, thereby increasing the calculated aspect ratio. We also note that our calculations predict an equilibrium shape, in which the base is *not* flat, but like a faceted dome even when only two tilted families of planes, {11$\bar{2}$1} and {10$\bar{1}$1}, are included. This is in agreement with the experimental observation on macroscopic Si$_3$N$_4$ matrix grains embedded in the intergranular phase, where the basal planes look atomically rough.[10]

It is particularly interesting to notice that of the two lowest-index prismatic planes rotated by 30° with respect to each other, it is the (11$\bar{2}$0) surface that is exposed in the Wulff construction and *not* the (10$\bar{1}$0) surface with open hexagonal rings, which has been shown to exhibit an abrupt interface with the rare-earth oxide additive in recent STEM experiments. The reason for the significantly lower surface energy of (11$\bar{2}$0) (1.95 J/m^2) compared to (10$\bar{1}$0) (2.57 J/m^2) can be understood from the nature of the atomic relaxations and the way the dangling bonds of Si are saturated. On the ideal (unrelaxed) (10$\bar{1}$0) surface, there are one Si and one N atom, which have one dangling bond each. These are shown by Si2 and N1 in Fig 3(a). When the surface is relaxed, while N1 still remains with a dangling bond, Si2 undergoes a considerable displacement ($\sim$0.8 Å) forming a new Si-Si bond with Si4 at 2.58 Å, only 10% larger than the bulk Si-Si distance [Fig. 3(b)]. As such, the dangling bond of Si2 is saturated, and the five-fold coordinated Si4 atom has two resonant bonds, reminiscent of overcoordination of Si in negatively charged E-center defect.[11] The surface is still somewhat rough due to the presence of the Si1-N1 unit, which does not relax significantly. On the ideal (11$\bar{2}$0) surface, on the other hand, there are two Si and two N atoms with one dangling bond each, labeled by Si6, Si4, N5, and N3 in Fig. 3(c). When this surface is relaxed, the resulting atomic displacements for most of the atoms are very
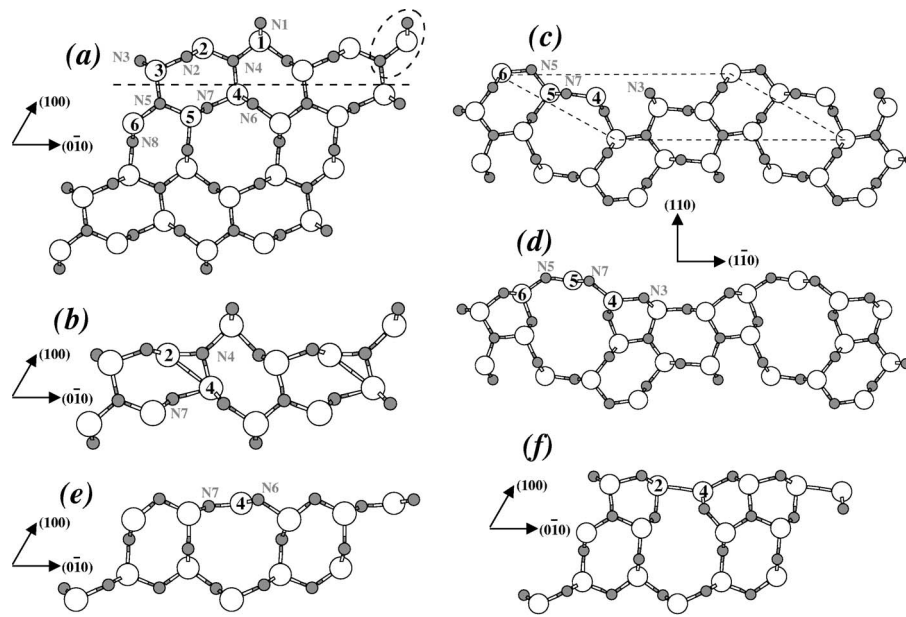
FIG. 3. [0001] projected, double-unit-cell views of (a) a two-layer ideal (10$\bar{1}$0) open-ring surface, (b) the top layer of the relaxed open-ring surface, (c) the two-layer ideal (11$\bar{2}$0) surface, (d) two-layer relaxed (11$\bar{2}$0) surface, (e) top layer of the relaxed half surface, and (f) relaxed structure of a nonstoichiometric (10$\bar{1}$0) surface with a missing SiN$_2$ unit (1.5 layers shown). In (a), the index 1, for example, inside a white circle denotes the Si1 atom mentioned in the text. If the atoms above the dashed line are removed, the ideal half surface is obtained. If the atoms inside the dashed ellipse (N1, Si1, and N4) are removed, the ideal structure of the nonstoichiometric surface (mentioned in the text) is obtained. In (c), the dashed region corresponds to a single unit cell of the (11$\bar{2}$0) surface.

large. For example, the displacements of N7, Si5, and Si6 are 1.51, 1.49, and 1.33 Å, respectively. Such large relaxations saturate all the dangling bonds except for N3, resulting in a rather smooth surface with seven-fold, three-fold, and four-fold Si-N rings [Fig. 3(d)]. The only undercoordinated Si atom on the relaxed surface (Si5 with no dangling bonds on the ideal surface) exhibits an sp^2-type bonding in an almost planar coordination with three N atoms.

We also investigated the relative structural stability of the (10$\bar{1}$0) bare surface as a function of stoichiometry. The formation energy of a surface, E_{form}, can be written as[12]

$$E_{\text{form}} = E_{\text{slab}}^{\text{tot}} - n_{\text{Si}}\mu_{\text{Si}} - n_{\text{N}}\mu_{\text{N}}, \qquad (1)$$

where $E_{\text{slab}}^{\text{tot}}$ is the total energy of the slab, n_i is the number of atoms of type i in the slab, and μ_i's are the corresponding chemical potentials, which satisfy $3\mu_{\text{Si}} + 4\mu_{\text{N}} = \mu_{\text{Si}_3\text{N}_4,\text{bulk}}$. Figure 4 shows the calculated energies as a function of the stoichiometry of the surface. All energies are relative to the stoichiometric surface with open hexagonal rings, which we will refer to as the "open-ring surface." This reference configuration is quite stable in the full allowed region of μ_{N} with the exception of two other terminations. The first one, which we will refer to as the "half surface," is obtained by removing half the atoms from the open-ring surface as shown by the dotted line in Fig. 3(a). This surface, while stoichiometrically terminated and quite smooth even in its ideal structure, does not have the open hexagonal rings, which are present at the Si$_3$N$_4$ rare-earth oxide interfaces studied in recent STEM experiments. When relaxed, the half surface becomes 0.17 eV (GGA) and 0.1 eV (LDA) lower in energy compared to

the open-ring surface. The only significant relaxation occurs for the Si atom (Si4) with the dangling bond that moves inward by $\sim$0.64 Å. As a result, the Si atom exhibits an sp^2-type bonding in a nearly planar coordination with three N atoms [Fig. 3(e)]. One possibility for the discrepancy between the theoretical prediction of the half surface having a lower energy than the experimentally observed open-ring surface at the rare-earth oxide interface is that theory incorrectly predicts the lowest energy termination of the bare
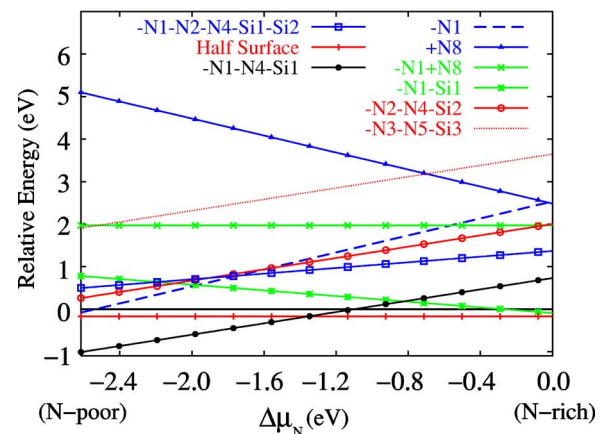

FIG. 4. (Color online) The formation energies of various terminations of the (10$\bar{1}$0) surface relative to the open-ring surface as a function of stoichiometry $\Delta\mu = \mu_{\text{N}} - 1/2\mu_{\text{N}_2}$. The (+) and (−) signs correspond to taking out and adding the particular atom, respectively, from the open-ring surface shown in Fig. 3(a) with all the atom indices.

$(10\bar{1}0)$ Si$_3$N$_4$ surface. This could be verified by studying the bare surface with low-energy electron diffraction experiments. A more likely reason for the discrepancy, which would also explain the prediction of the $(11\bar{2}0)$ surface as the lower-energy prismatic plane contrary to experimental observations, is that the rare-earth oxide additive changes the relative stability of different Si$_3$N$_4$ surfaces and different terminations of the same-index surfaces.

The second termination, which results in a lower energy surface under N-poor conditions, is obtained by removing a SiN$_2$ unit (N1, N4, Si1) from the open-ring surface, as shown by the dashed ellipse in Fig. 3(a). In its ideal structure, this surface has two Si atoms, Si4 and Si2, with one and two dangling bonds, respectively, along with a N atom (N3) with one dangling bond. In spite of a large number of broken bonds, when the surface is relaxed, large atomic displacements of Si2 (1.29 Å) and Si4 (1.27 Å) saturate all Si dangling bonds (via the formation of a new Si–Si bond at 2.5 Å), which reduces the surface energy considerably. The relaxed surface is smooth and has seven-fold and three-fold rings, similar to those observed on the $(11\bar{2}0)$ surface [Fig. 3(f)]. It is interesting to note that under extreme N-poor conditions, the energy of this surface is 1.85 J/m^2, which is lower than that of $(11\bar{2}0)$, providing a possible explanation for the dominant observation of $(10\bar{1}0)$ surfaces in the STEM experiments.

In summary, we have presented results from *ab initio* calculations on the atomic and electronic structures of bare β-Si$_3$N$_4$ surfaces with emphasis on the prismatic plane $(10\bar{1}0)$ surface observed in recent STEM experiments. The equilibrium shape of a macroscopic Si$_3$N$_4$ crystal is found to have a hexagonal cross section, a faceted domelike base, and an aspect ratio of 1.4, in agreement with experimental observations. We find large distortions on the prismatic planes driven primarily by the tendency of Si atoms to saturate their dangling bonds and achieve either resonant bond, sp^3- or sp^2-bonded configurations. The stoichiometric $(11\bar{2}0)$ surface, the $(10\bar{1}0)$ half surface, and a nonstoichiometric $(10\bar{1}0)$ surface obtained by removing a SiN$_2$ unit are predicted to have lower energies than the open-ring $(10\bar{1}0)$ surface. In light of the consistent experimental observations of the open-ring $(10\bar{1}0)$ surface at the interface, the present results obtained with state-of-the-art *ab initio* techniques strongly indicate that (i) the rare-earth oxide additive changes the relative stability of β-Si$_3$N$_4$ surfaces, and (ii) nonstoichiometry (especially resulting from N-poor conditions) should play an important role in determining the termination of the Si$_3$N$_4$ matrix grains. We expect that future *ab initio* studies of the interface will not only focus on the bonding nature of the additives to the open-ring $(10\bar{1}0)$ surface, but also address why the proposed mechanisms do not favor promotion of the $(11\bar{2}0)$ termination, which has a lower bare surface energy.

[1] M. J. Hoffmann, in *Tailoring of Mechanical Properties of Si₃N₄ Ceramics*, edited by M. J. Hoffmann and G. Petzow (Kluwer, Dordrecht, 1994), p. 59.

[2] E. Y. Sun *et al.*, J. Am. Ceram. Soc. **81**, 2831 (1998); R. L. Satet and M. J. Hoffmann, J. Eur. Ceram. Soc. **24**, 3437 (2004).

[3] N. Shibata *et al.*, Nature **428**, 730 (2004); A. Ziegler *et al.*, Science **306**, 1768 (2004); G. B. Winkelman *et al.*, Philos. Mag. Lett. **84**, 755 (2004).

[4] P. Rulis *et al.*, Phys. Rev. B **71**, 235317 (2005); G. S. Painter *et al.*, *ibid.* **70**, 144108 (2004); M. Yoshiya *et al.*, J. Am. Ceram. Soc. **85**, 106 (2002); T. Nakayasu *et al.*, *ibid.* **81**, 565 (1998); P. Dudešek and L. Benco, *ibid.* **81**, 1248 (1998); L. Benco, Surf. Sci. **327**, 274 (1995).

[5] G. Kresse and J. Hafner, Phys. Rev. B **47**, R558 (1993); P. E. Blöchl, *ibid.* **50**, 17953 (1994).

[6] A. Y. Liu and M. L. Cohen, Phys. Rev. B **41**, 10727 (1990); R. Belkada, T. Shibayanagi, and M. Naka, J. Am. Ceram. Soc. **83**, 2449 (2000).

[7] P. Villars, *Pearson's Handbook of Crystallographic Data for Intermetallic Phases* (ASM International, Materials Park, Ohio, 1995).

[8] D. R. Clarke, J. Am. Ceram. Soc. **70**, 15 (1987); H. J. Kleebe *et al.*, *ibid.* **76**, 1969 (1993).

[9] G. Wulff, Z. Kristallogr. Mineral. **34**, 449 (1901).

[10] M. Krämer *et al.*, J. Cryst. Growth **140**, 157 (1994).

[11] S. Öğüt and J. R. Chelikowsky, Phys. Rev. Lett. **91**, 235503 (2003).

[12] G.-X. Qian, R. M. Martin, and D. J. Chadi, Phys. Rev. B **38**, 7649 (1988).